Kinetics of Atomic Cascade in Light Exotic Atoms

V.E. Markushin [a] and T.S. Jensen [a,b]

[a] *Paul Scherrer Institute, CH-5232 Villigen, Switzerland*
[b] *Institut für Theoretische Physik der Universität Zürich, Switzerland*

Recent results on the kinetics of atomic cascade in hydrogen–like exotic atoms are reviewed. The problem of kinetic energy distribution during the atomic cascade is studied in detail with a new Monte Carlo kinetics code. For the first time, nuclear absorption in the light hadronic atoms is treated consistently with elastic scattering and Stark mixing processes by using the collisional cross sections calculated in the close–coupling approximation [1]. The rates for the high n states are calculated with the classical–trajectory Monte Carlo method. Evidences for cascade processes beyond the extended standard cascade model are discussed.

Keywords: exotic atom, muonic hydrogen, pionic hydrogen, cascade, kinetics.

1. Introduction

The standard cascade model (SCM) of light exotic atoms originally introduced by Leon and Bethe [2] was further developed during the past decade in order to describe acceleration and deceleration effects [3,4]. The studies done with the extended standard cascade model (ESCM) were strongly stimulated by the experiments in which the energy distribution of $\pi^- p$, $\mu^- p$, and $\mu^- d$ atoms was measured using various time-of-flight methods [5–10]. The possibility to get detailed information on the evolution of the kinetic energy distribution during the atomic cascade in addition to the standard observables, such as X-ray yields and cascade times, gives us interesting opportunities to investigate various reactions with exotic atoms in excited states. A number of experiments on precision spectroscopy of $\mu^- p$, $\pi^- p$, $\pi^- d$, and $K^- p$ [10–12] crucially rely on a good knowledge of the kinetic energy distribution and a good understanding of related cascade mechanisms. This challenge must be responded with an adequate cascade model of ab initio type, possibly including some processes beyond ESCM. The goal of this paper is to review the recent progress in this field since the EXAT-98 Conference (see [13] and references therein).

2. Cascade Mechanisms

The extended standard cascade model [3] takes into account the interaction between internal and external degrees of freedom of the exotic atom; the kinetic energy distribution changes during the cascade due to competition between the acceleration and deceleration mechanisms. In the present version of our cascade model, a significant improvement over the previous calculations is achieved by using a new set of differential cross sections of the collisional processes

$$(x^-p)_{nl} + \mathrm{H} \to (x^-p)_{nl'} + \mathrm{H} \quad x^- = \mu^-, \pi^-, K^-, \bar{p} \tag{1}$$

$$(x^-p)_{nl} + \mathrm{H}_2 \to (x^-p)_{nl'} + X \quad X = \mathrm{H}_2,\ \mathrm{H}+\mathrm{H} \tag{2}$$

calculated in self–consistent ways using the close–coupling method for low n states and the classical–trajectory Monte Carlo method for high n states, see [1] for details. This allows us to describe the competition between deceleration and Stark mixing, as well as the absorption in hadronic atoms due to Stark collisions, without employing any fitting parameters related to the Stark mixing and deceleration, like k_{Stk} used in many earlier calculations.

Concerning the acceleration mechanisms, the present calculations include Coulomb deexcitation through the whole cascade. For high n states ($n \geq 8$), the classical–trajectory Monte Carlo method was used to obtain the cross sections of the inelastic collisions [1]

$$(x^-p)_{n_i} + \mathrm{H}_2 \to (x^-p)_{n_f} + X \quad X = \mathrm{H}_2,\ \mathrm{H}_2^*,\ \mathrm{H}+\mathrm{H} \quad . \tag{3}$$

The Coulomb transitions ($n_f < n_i$) in collisions with molecules were found to be the dominant deexcitation mechanism at high n with a typical cross section of a few atomic units. In the beginning of the cascade, the most probable transitions are the ones with $\Delta n > 1$ leading to H_2 excitation or dissociation. The latter corresponds to the so-called chemical deexcitation introduced for phenomenological reasons in the old standard cascade model. For low n states, where a quantum–mechanical description is required and molecular effects are possibly important, we could not avoid introducing effective Coulomb deexcitation rates which were tuned to reproduce the π^-p data.

One of the goals of the present calculations is to confront ESCM with the experimental data and to determine the domains of agreement and disagreement in order to identify possible significant mechanisms beyond ESCM. Some candidates for such mechanisms are known to be related to the formation of molecular resonances in excited states (see [14,15] and references therein).

3. Muonic hydrogen

The calculated relative X-ray yields for the μ^-p atom are in a good agreement with the experimental data, see Fig. 1a. At high density, a significant

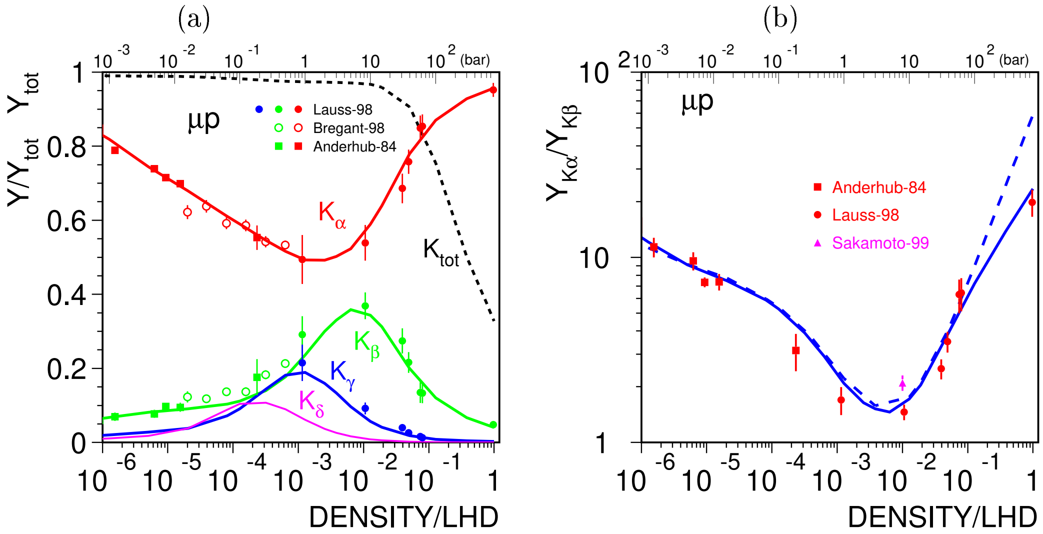

Figure 1. (a) The density dependence of the relative X-ray yields (solid lines) and the absolute total yield $K_{\mathbf{tot}}$ (dashed line) in muonic hydrogen. The experimental data are from [16–18]. (b) The ratio of the K_α and K_β yields for the nonradiative (solid line) and radiative (dashed line) quenching of the $2S$ state. The data are from [16,17,19].

fraction of the μ^-p atoms slows down at the very end of the cascade before reaching the ground state and populates the metastable $2S$ state with high probability ($p_{2S}^{\rm init} \approx 0.7$ in liquid hydrogen). This makes the ratio of K_α and K_β yields in liquid hydrogen very sensitive to a quenching mechanism of the $2S$ state. As demonstrated in Fig. 1b, the X-ray data favor nonradiative quenching in agreement with the recent experiment on direct search for the metastable $2S$ state [9]. It would be extremely important to check this result directly by measuring the *absolute* X-ray yield in liquid hydrogen: the nonradiative quenching leads to a significant suppression of the X-ray yield $Y_{K_{\rm tot}} \approx 0.3$.

The initial population and the initial energy distribution of μ^-p atoms after their formation can be studied by measuring the energy distribution at the end of the cascade at low density. The new PSI data [9,10] are in fair agreement with the cascade calculations assuming that the initial n-distribution is peaked around $n = 13$ and the average initial kinetic energy is about 0.5 eV, see Fig. 2a. The data at 0.06 mb are mainly sensitive to the initial energy distribution. With the density increasing, the final distribution becomes more energetic due to acceleration at the beginning of the cascade. In the density range shown in Fig. 2a, the Coulomb transitions with $\Delta n > 1$ were found to be essential for this acceleration in agreement with the earlier analysis [8].

The energy distributions at the low part of the cascade can be determined by measuring the Doppler broadening of the X-ray lines [3], the experiment being currently in progress at PSI [11]. In the present calculations, we used the effective Coulomb deexcitation rates for $n \leq 7$ which were normalized using the π^-p

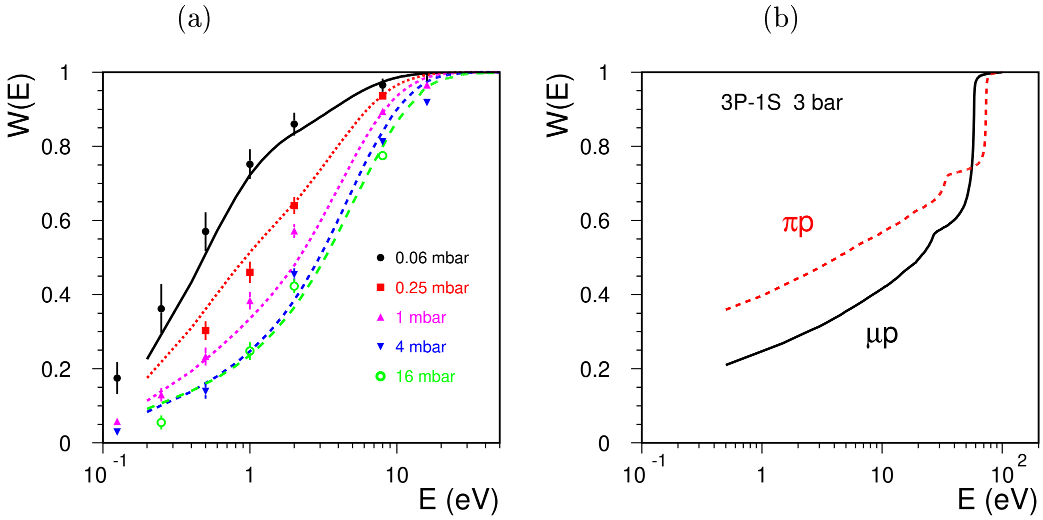

Figure 2. (a) The cumulative energy distribution $W(E)$ of the μ^-p atom at the end of the cascade. The data are from [9]. (b) The cumulative energy distribution of μ^-p (solid line) and π^-p (dashed line) at the instant of the $3P-1S$ transition at 3 bar.

data (see Sec. 4). The calculated energy distributions of μ^-p during the radiative transitions $nP-1S$ have significant high–energy components resulting from the preceding Coulomb–like transitions, as shown in Fig. 2b. The experimental verification of these results will provide a direct determination of the strength of the Coulomb–like acceleration mechanisms and may help to uncover the dynamics of these processes at low n.

4. Pionic hydrogen

The results of our cascade calculations for the X-ray yields and the energy distribution at the instant of the nuclear reaction $\pi^-p \to \pi^0 + n$ are shown in Fig. 3. Because we consider the calculations of the direct collisions $\pi^-p + \mathrm{H}$ [1] and the corresponding Stark mixing, absorption, and deceleration rates sufficiently reliable, we do not use any tuning parameters related to these processes. Since it was found that the rates corresponding to the adiabatic mechanism of the Coulomb transitions [7] are too small to explain the observed high–energy component in the π^-p data, a phenomenological description of the Coulomb–like acceleration was used in the present calculations. It turned out that a parametrization close to the semiclassical estimate by Bracci and Fiorentini [21] can provide a fair description of the data on the π^-p energy distribution. Furthermore, we found that the standard mechanisms of absorption related to direct Stark mixing are not sufficient to explain the measured density dependence of the absolute X-ray yields (the same problem existed in all previous calculations where it was usually cured by ad hoc enhancement of the Stark mixing rates). We could get a better

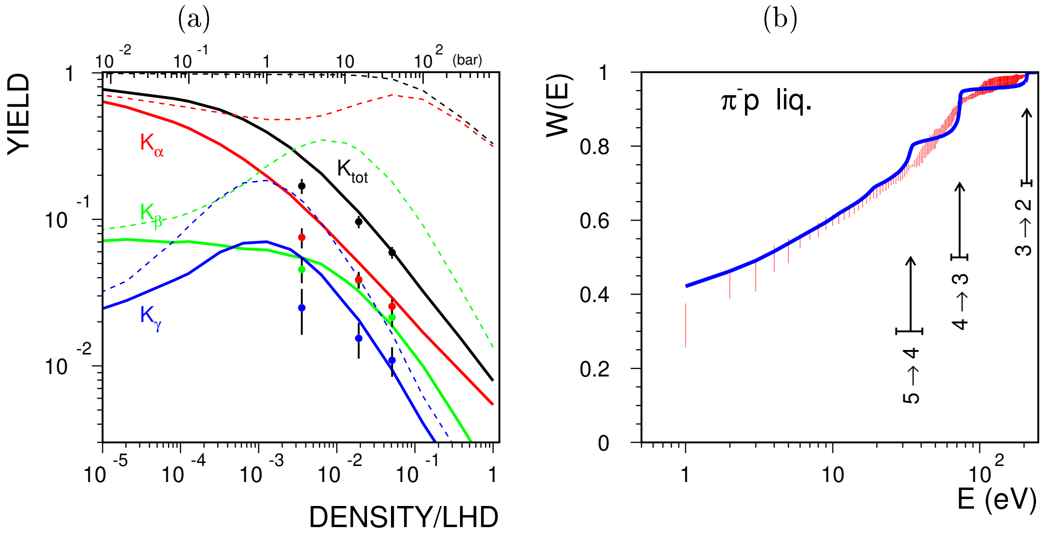

Figure 3. (a) The density dependence of the absolute X-ray yields (solid lines) in pionic hydrogen. The data are from [20]. The dashed lines show the corresponding yields in muonic hydrogen. (b) The calculated cumulative energy distribution $W(E)$ of the π^-p atom at the instant of nuclear reaction in liquid hydrogen (solid line) in comparison with the data [7]. The kinetic energies corresponding to the Coulomb transitions $n_i \to n_f$ are shown by arrows, with horisontal bars indicating the energy resolution of the measurement [7].

agreement with the data by introducing an additional absorption mechanism at low energy $E \leq 1$ eV for $n = 2, 3, 4, 5$ with a characteristic rate about one half of the effective Stark mixing $nl \to nS$. We consider the necessity of this adjustment as an evidence for additional absorption mechanisms, possibly related to the formation of molecular resonances in excited states [14,15]. The details of the cascade calculations and further discussion will be published elsewhere.

The kinetic energy distribution of π^-p at the instant of the K_β transition is shown in Fig. 2b in comparison with that of μ^-p at the same target density. Since the cascade processes in these two cases are very similar, except for the absorption, there is a strong correlation between the corresponding kinetic energy distributions. This is very important for the calculation of Doppler broadening corrections to the width of the $1S$ state of pionic hydrogen [11] because the muonic hydrogen data can be used as an additional test of the cascade model involved.

5. Conclusion

The present version of our cascade model contains significant improvements over the previous calculations due to the self–consistent treatment of elastic scattering, Stark mixing, and nuclear absorption. The evolution of the kinetic energy distribution is calculated from the very beginning of the cascade.

By confronting the predictions of the extended standard cascade model with the experimental data we can identify a few evidences for processes beyond ESCM. One case is related to the nonradiative quenching of the metastable $2S$ state in muonic hydrogen, which appears to be related to the formation of molecular resonances [9,15]. As the adiabatic Coulomb deexcitation [22] is not sufficiently strong to explain the observed kinetic energy distribution of π^-p at the instant of the nuclear reaction, further detailed studies of Coulomb–like acceleration via the formation of excited molecular states [14] at $n = 2 - 6$ are required. The same mechanism may also be responsible for the additional absorption of π^-p atoms at low energy, which we found to be needed in addition to the direct Stark mixing mechanisms. We plan to include an explicit treatment of these processes in the next version of our cascade code.

Acknowledgements

We thank M. Daum, P. Hauser, F. Kottmann, R. Pohl, L. Simons, J. Schottmüller, and D. Taqqu for fruitful and stimulating discussions. One of the authors (V.M.) thanks Prof. K. Nagamine and RIKEN for the support of his participation in the μCF-01 Conference.

References

[1] T.S. Jensen and V.E. Markushin, Nucl. Phys. A **689** (2001) 537; this issue.
[2] M. Leon and H.A. Bethe, Phys. Rev. **127** (1962) 636.
[3] V.E. Markushin, Phys.Rev. A **50** (1994) 1137.
[4] E.C. Aschenauer et al., Phys. Rev. A **51** (1995) 1965.
[5] J.E. Crawford et al. Phys. Lett. **213B** (1988) 391; Phys. Rev. D **43** (1991) 46.
[6] D.J. Abbott et al., Phys. Rev. A **55** (1997) 165.
[7] A. Badertscher et al., Europhys. Lett. **54** (2001) 313.
[8] F. Kottmann et al., Hyperfine Interactions **119** (1999) 3.
[9] R. Pohl et al., this issue; R. Pohl, Diss. ETH No. 14096, Zürich, 2001.
[10] F. Kottmann et al., this issue.
[11] D. Gotta et al., this issue; D. Gotta, πN Newsletter **15** (1999) 276.
[12] The DEAR Collaboration, R. Baldini et al., Preprint LNF-95/055 (1995).
[13] V.E. Markushin, Hyperfine Interactions **119** (1999) 11.
[14] S. Jonsell, J. Wallenius, P. Froelich, Phys. Rev. A **59** (1999) 3440.
[15] J. Wallenius, this issue.
[16] A. Anderhub et al., Phys. Lett. **143B** (1985) 65.
[17] B. Lauss et al., Phys. Rev. Lett. **80** (1998) 3041.
[18] M. Bregant et al., Phys. Lett. A **241** (1998) 344.
[19] S. Sakamoto et al., Phys. Lett. A **260** (1999) 253.
[20] A.J. Rusi El Hassani et al., Z. Phys. A **351** (1995) 113.
[21] L. Bracci and G. Fiorentini, Nuovo Cim. **43A** (1978) 9.
[22] L.I. Ponomarev, E.A. Solov'ev, Hyperfine Interactions **119** (1999) 55.